Effects of the Excitation Wavelength on the SERS Spectrum

ARTICLE *in* JOURNAL OF PHYSICAL CHEMISTRY LETTERS · APRIL 2012

Impact Factor: 7.46 · DOI: 10.1021/jz201625j

1 AUTHOR:

Ramón A Alvarez-Puebla

Catalan Institution for Research and Advance…

141 PUBLICATIONS **5,091** CITATIONS

SEE PROFILE

THE JOURNAL OF PHYSICAL CHEMISTRY Letters

Perspective

pubs.acs.org/JPCL

Effects of the Excitation Wavelength on the SERS Spectrum

Ramón A. Álvarez-Puebla*

Departamento de Química Física, Universidade de Vigo, 36310 Vigo, Spain

ABSTRACT: SERS is nowadays a well-established ultrasensitive technique with potential to solve many analytical problems, especially those related to biosciences. This Perspective article aims at summarizing the experimental complexities, in particular, those related to the interaction of light with the sample, that the SERS practitioner may find when acquiring a spectrum while providing a general basis for the interpretation of the obtained vibrational features. With such an idea in mind, factors related to the instrumentation, the optical enhancer, and the analyte molecule are discussed to illustrate the effects of the incident light on the absolute and relative intensity, as well as the spectral profile of the SERS spectra.

Surface-enhanced Raman scattering (SERS) spectroscopy is a linear Raman technique carried out on nanostructured plasmonic materials. Upon excitation with the appropriate light, the nanomaterial generates a strong electric field that couples with the vibrational modes of the molecule under study, increasing its characteristic signals and making possible its ultrasensitive or even single-molecule detection.[1] In fact, SERS is becoming one of the most popular ultrasensitive analytical techniques especially in academia but with a number of real-life applications developed on a daily basis in different fields including environmental monitoring,[2] biology, or medicine.[3] The analytical potential and versatility of this technique make it applicable in almost any analytical matrix and, more importantly, with minimum or no sample preparation at all and under the natural chemical and thermodynamic conditions of the analyte under study.

The main mechanism of SERS is electromagnetic in nature.[4−6] When photons of the appropriate energy excite a plasmonic nanostructure, the electric field of the radiation drives the conduction electrons into collective oscillations, generating the so-called localized surface plasmon resonances (LSPRs). The excitation of the LSPR has two main consequences, the selective absorption and scattering of the resonant radiation and the generation of gigantic electromagnetic fields at the surface of the nanostructure.[7] In Raman scattering, the intensity of the scattered radiation is proportional to the square of the magnitude of the electromagnetic field incident on the analyte ($I \alpha E_0^2$). However, in SERS, due to the close proximity of a plasmonic nanostructure with the analyte, the electromagnetic field is not only the incident field but also that generated by the LSPR (eq 1)

$$|E_{out}|^2 = 4E_0^2\left(\frac{\varepsilon_{in} - \varepsilon_{out}}{\varepsilon_{in} + 2\varepsilon_{out}}\right)^2 \quad (1)$$

where ε_{in} is the dielectric constant of the metal nanoparticle and ε_{out} is that of the external environment. Thus, for a given excitation wavelength, the SERS intensity is related to the absolute square electromagnetic field outside of the particle and is enhanced, with respect to the Raman intensity, by a factor (EF), as described in eq 2

$$EF_{(\lambda)} = \frac{|E_{out(\lambda)}|^2|E_{out(\lambda-\lambda s)}|^2}{E_0^4} = \frac{I_{SERS}}{I_R}f \quad (2)$$

where $E_{out(\lambda)}$ and $E_{out(\lambda-\lambda s)}$ are the electromagnetic fields generated by the incident excitation and the Stokes's shifted Raman. The use of the first term of eq 2 for the calculation of the enhancement factor (EF) is difficult; thus, experimentally, EFs are usually calculated by direct comparison of the intensities provided by the SERS and Raman experiments and normalized by the total number of molecules (N) in each experiment ($f = N_R/N_{SERS}$).

The other mechanism that yields enhancement, and is complementary to the electromagnetic, is the so-called chemical or charge-transfer (CT) mechanism.[8,9] CT is related to the chemical complexation of the analyte molecules to the surface of the metallic nanostructure. In this situation, the laser excitation brings about the possibility of a CT excitation, which in the case of SERS could be molecule-to-metal or metal-to-molecule, a transition between the Fermi level of the metal nanostructure and the lowest unoccupied molecular orbital (LUMO) of the adsorbed molecule. Although the chemisorption of the analyte may change the vibrational pattern due to the change in the molecular symmetry, molecular orientation on the surface, and light polarization at the surface of the nanostructure, the CT may also leads to lager EFs generated by a resonance Raman effect due to excitation into a CT transition.

While these two mechanism are a matter of continuous interest and extremely interesting material can be found in the literature,[4−6,8,9] several other factors such as the effects of the excitation light on the molecular system under study, and therefore on the obtained SERS spectrum, are usually partially described. In fact, common questions of novel users include: Why use more than one excitation wavelength for the characterization of a given analyte, how to select the most appropriate excitation wavelength for a given application, why the

Received: December 10, 2011
Accepted: March 8, 2012
Published: March 8, 2012

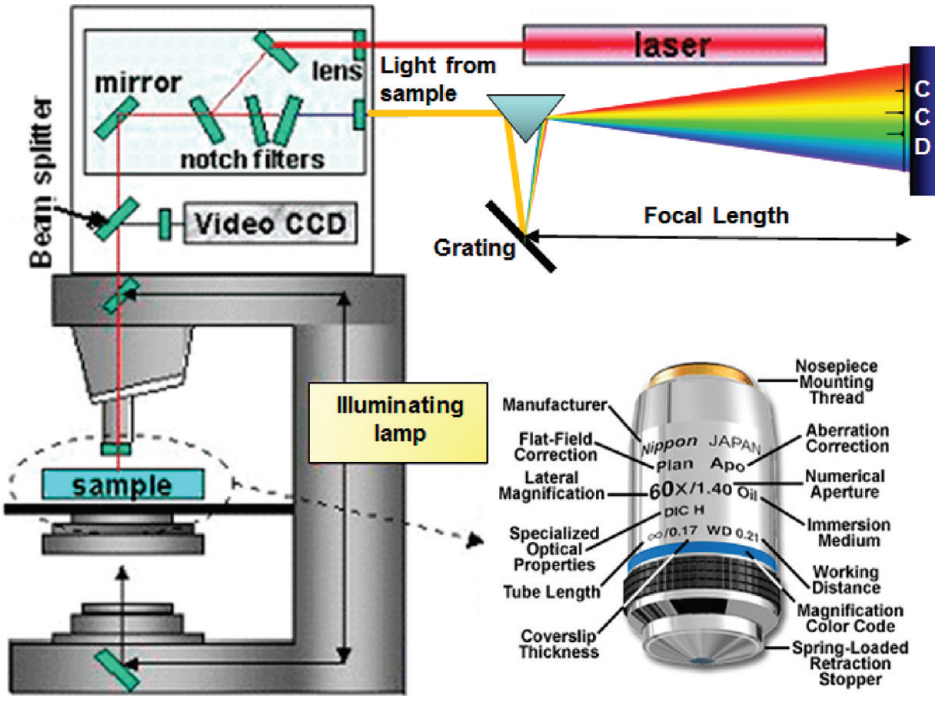

Figure 1. Schematic description of a dispersive Raman microscope comprised of a confocal optical microscope with a video camera, excitation light (lasers), highly efficient optics (mirrors, notch or edge filters, and optical lenses), monochromator (grating), and detector (CCD). The description of a microscope objective is also shown.

spectra of some molecule changes as a function of the excitation wavelength, why the SERS signal is high when using excitation lines, a priori, far away from the localized plasmon resonance, and how to know and identify photoeffects (photodegradation, photocatalysis, photobleaching, or photodesorption) acting on the analyte, among others. This Perspective aims at responding to these questions and giving a clear idea for the selection of the appropriate wavelength to excite the analyte as a function of its chemical nature and the desired application. Further, the effects of light on the absolute and relative intensity and spectral profile for the SERS spectrum will be analyzed in light of (i) the instrumentation, (ii) the optical enhancer, and (iii) the analyte under study.

Instrumentation. Excitation Sources (Lasers). As all spectroscopies, SERS requires the illumination of the sample with light. SERS, as Raman scattering, relies on the collection of the inelastically scattered part of the incident monochromatic excitation. The light interacts with the molecular analyte, exciting electrons from the ground state to the vibrational levels; this results in an energy shift of some photons, which correlates with the vibrational modes of the system. This effect, the inelastic scattering, is extremely inefficient, and excitation of the sample requires the use of intense light sources (i.e., lasers). Common excitation sources include radiation from the UV to the NIR, and several lines can be found mounted in the same dispersive Raman system. The selection of one laser source or another depends strictly on the application. For example, 244 nm is widely used in resonance Raman scattering characterization of biological structures, whereas 325 nm is used in the electronic and semiconductors industries, visible lines (488, 514, 532, and 633 nm) are general purpose, and NIR lines (785 and 830 nm) find a place in general, biological, and medical fields, especially for samples with native fluorescence in the visible and those that photodegrades easily. All of these sources can be applied to produce SERS; notwithstanding, UV lasers have been demonstrated to yield very modest enhancements as compared with those in the visible and NIR.[10] Therefore, in SERS experiments, excitation is almost restricted from the blue to the NIR. It should also be considered that as the laser wavelength gets shorter, the Raman scattering efficiency increases, but also the risk of fluorescence, the sample damage, and the cost of the spectrometer increase.

Objectives. Classically, sample excitation in Raman systems has been carried out in 90° geometries to avoid the excitation of the detector with the Rayleigh radiation. Due to the advances in optics, highly efficient holographic notch filters and special dielectric mirror filters are now available at affordable prices. Thus, modern dispersive Raman instruments are usually attached to microscopes, where the excitation and the inelastically scattered light is delivered to, and collected from, the sample through the same objective in a backscattering geometry (180°), as shown in Figure 1. The use of a microscope permits a dramatic increase in the spatial resolution, minimal depth of field, and the highest possible laser energy density for a given laser power. The diameter of the airy disk formed by a laser focus (d) is often affected by the improper matching of the laser size to the back-aperture of the objective and by the wavefront errors inherent to the laser and/or introduced by the laser delivery optics. However, without consideration of the laser mode quality and wavefront, d depends, essentially, on two factors, the numerical aperture (N.A.) of the objective, which characterizes the range of angles (γ) over which the system can accept or emit light, and the energy of the excitation line (λ) as noted in eq 3

$$d = \frac{1.22\lambda}{\text{N.A.}} \tag{3}$$

The laser focused spot size does not necessarily define the lateral spatial resolution of the Raman system. For the collected light, the lateral spatial resolution is often discussed in terms of

dx.doi.org/10.1021/jz201625j | J. Phys. Chem. Lett. 2012, 3, 857–866

the Rayleigh criterion. For the resolution of two adjacent point sources of light of the same intensity, this criterion requires that the principal diffraction maximum of one image coincide with the first minimum of the other. Thus, the distance between the two points needs to be greater than the distance from the peak to the first airy disk minimum. Complete discrimination of two adjacent points occurs at twice the Rayleigh criterion. Thus, the maximum achievable spatial resolution is given by the radius (r) of the airy disk, eq 4

$$r = \frac{d}{2} = \frac{1.22\lambda}{2\text{N.A.}} \tag{4}$$

Table 1 shows the minimum lateral resolution for two different lines as a function of the objective used for the excitation/collection. As noted in eq 4, the spatial resolution depends exclusively on the excitation line (i.e., more energetic photons will yield higher resolution) and on the N.A. of the objective. However, although multiple objectives may be available with the same N.A. but differing magnifications for a given manufacturer, commonly, the increase in the augments of an objective increase also the N.A. Thus, for conventional objectives, such as those described in Table 1, the spatial resolution augments with the magnification. It is important to note as well that the objective used to deliver the light also affects the laser energy density and thus the spectral intensity. The calculation of the relative intensity airy profiles[11] for a 514 nm wavelength (Figure 2A) makes clear that decreasing the augments of the objective severely decreases the energy density at the sample. This effect has a direct impact on the experimental acquisition (Figure 2B), where the SERS intensity of benzenethiol (BT) was reduced around 50% by just changing a ×50 objective for a ×20 and more than 80% when the objective used was the ×5.

Table 1. Dependence of the Lateral Spatial Resolution of the Augments of Conventional Objectives for Two Laser Lines at 514 and 785 nm

objective augments	N.A.	2γ/deg	d (514 nm)/μm	r (785 nm)/μm
×5	0.12	11.5	2.72	4.15
×20	0.4	29	0.82	1.99
×50	0.75	97.2	0.44	0.66
×100	0.9	128.3	0.36	0.55

The depth of field penetration of the laser into the sample (h) is determined by the excitation line (λ), the refractive index of the surrounding media (n), and the N.A. (eq 5), while the illuminated volume (V), when using a macrosampling objective, is defined by the focal length (f) and the lens diameter (D), where f/V represents the aperture angle, equivalent to the N.A. (eq 6)

$$h = n\frac{\lambda}{\text{N.A.}^2} \tag{5}$$

$$V = 3.21\lambda^3\left(\frac{f}{D}\right)^4 \tag{6}$$

Thus, the excitation energy should be carefully considered for each application. For example, without other considerations such as damage at the sample, which will be discussed later, if working with thin films, a shorter wavelength excitation will be preferred to avoid contamination of the sample spectrum with the vibrational bands of the support. On the other hand, when working with colloidal solutions and a macrosampling objective, the preferred excitation would be that of larger wavelength to increase the volume sampled, decreasing in that case the signals from the vial containing the liquid.

With these parameters, spatial resolution and depth of field (or illuminated volume in the case of solutions), the calculation of the number of molecules sampled either in SERS or Raman is possible. In turn, the number of molecules sampled in the experiment is a necessary for the experimental calculation of EFs as requested in eq 2.

Grating. The ability to resolve features within the spectrum (i.e., spectral resolution) depends mainly on two factors, the density of grooves in the grating and the focal length between the grating and the detector (Figure 1). The spectral resolution is directly proportional to both of them and increases as both increase. However, while the focal length is usually fixed, modern instruments implement more than one grating because shorter wavelengths require higher levels of resolution while longer wavelengths cannot be resolved with high groove density gratings. The selection of one grating or another is not trivial either. The rule of thumb is, in this case, that higher groove density yields higher spectral resolution but lower spectral intensity and requires longer acquisition time. On particular occasions and depending on the application, it is not a bad idea to sacrifice resolution to gain intensity and therefore also time.

An alternative to gain intensity while preserving, or even increasing, resolution is the use of blazed gratings. Blazed gratings are manufactured to form right angles (i.e., the angular distance from the surface normal to the diffraction plate) for a

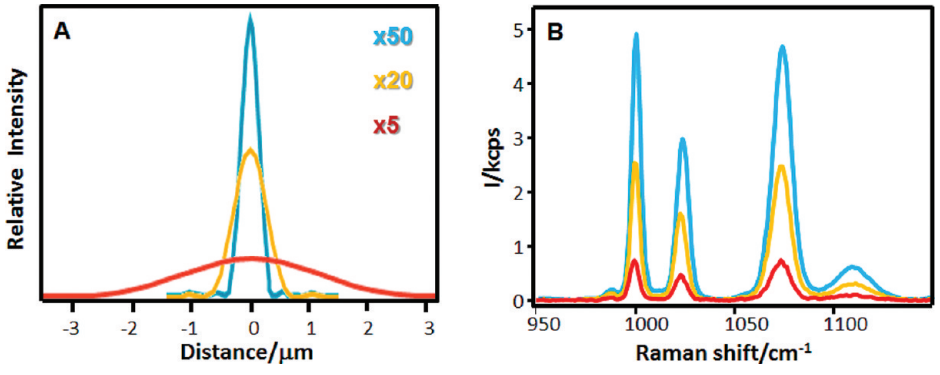

Figure 2. (A) Relative intensity profiles of an airy disk for an excitation light of 514 nm delivered with different conventional objectives, ×50 (N.A. 0.75), ×20 (N.A. 0.4), and ×5 (N.A. 0.12). (B) Experimental SERS spectra of BT supported on silver colloids upon excitation with a 514 nm laser with the same power at the sample but using different objectives.

dx.doi.org/10.1021/jz201625j | J. Phys. Chem. Lett. 2012, 3, 857–866

given wavelength. The magnitude of the blaze angle determines the wavelength at which the grating will be most efficient. Unfortunately, this blazing notably decreases the efficiency of the grating for other wavelengths, as in agreement with the rule of 2/3−3/2, which gives the range of use of the grating (lower limit = 2/3 blaze; upper limit = 3/2 blaze). Further, the intensity can be as well improved by using highly efficient mirror coatings. The efficiency of the grating is usually measured in the Littrow configuration for a given wavelength

$$\%\ \text{relative efficiency} = \frac{\text{Transmission grating efficiency}}{\text{Transmission mirror efficiency}} \cdot 100 \quad (7)$$

The simplest (and cheapest) optical coating is a thin film of Al, which yields a reflectivity of around 88−92% over the visible spectrum. Other usual coatings include Ag, which has a reflectivity of 95−99% even into the far-infrared but suffers from decreasing reflectivity (less than 90%) in the blue and UV spectral regions, and Au, which gives excellent reflectivity (98−99%) throughout the IR but limited reflectivity at wavelengths shorter than 550 nm.

Detector. Older spectrometers used photographic plates to detect the scattered light. The advent of more sensitive photomultiplier tubes has led to their widespread use, allowing the data to be collected and manipulated electronically. However, they have the key disadvantage of being only able to count photons with one wavelength at a time. Modern spectrometers use charge-coupled devices (CCDs) that combine the advantages of the previous techniques, being highly sensitive, electronic, and capable of measuring the whole spectrum at once. However, for different spectrometers and also for the same spectrometer working with different excitation lines, quantum efficiency of the detector varies, thus perturbing the true spectrum (intensity versus Raman shift). The resulting uncertainties in the relative intensity result from the fact that Raman spectroscopy is a single-beam technique lacking the internal response calibration inherent in absorbance measurements.

For different spectrometers and also for the same spectrometer working with different excitation lines, the quantum efficiency of the detector varies, thus perturbing the true spectrum (intensity versus Raman shift).

For the same sample excited with two different wavelengths, the shorter one will overestimate the intensity of the bands at high wavenumbers, while the longer one will do the same with the shorter wavenumbers (Figure 3). Several approaches have been developed to solve this detector artifact by using a "laser line fluorescence standard" and mathematical algorithms,[12] such as in the case of Figure 3. However, although the results are impressive, these approaches are not popular at all, and Raman/SERS spectra are usually published as obtained. Thus, the Raman and SERS practitioner should be aware of this effect to avoid misleading interpretations.

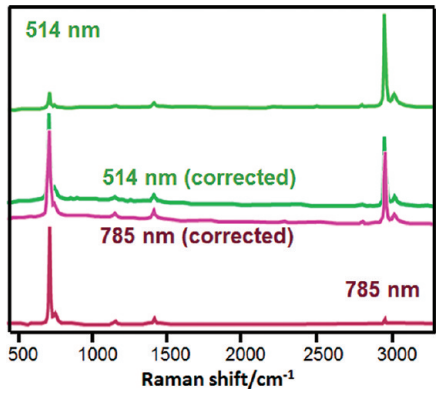

Figure 3. Raman spectra of CH_2Cl_2 obtained as excited with a 514 (top) or 785 nm (bottom) laser line and after correction with a tungsten bulb at 514 nm or a 2412 glass at 785 nm.

Optical Enhancers. Contrary to Raman scattering, SERS requires an optical enhancer to generate the electromagnetic field necessary to enhance the vibrational signal. This additional element introduces a new set of variables in the scenario such as LSPR excitation, thermal heating, photocatalysis, or hidden resonances. In this section, only the first effect will be discussed as the rest have been included in the last part of this Perspective. LSPR depends on the shape, size, composition, spatial organization, and dielectric environment of the plasmonic materials. In the early days of SERS, plasmonic materials were restricted to physically evaporated or electrochemically roughened noble metal thin films or to colloidal solutions of gold and silver. Thus, the plasmonic response in these optical enhancers was very restricted. Actually, the extreme advance in both lithography and wet chemical synthesis permits the preparation of nanomaterials with any desired optical response, through the control of their shape, size, and organization.[13−15] Figure 4A shows the LSPR variation of gold nanorods as they are grown and reshaped into octahedra.[16] This example illustrates the possibility of tuning the particle morphology to get the optical response in the desired spectral region. With this possibility at hand, the following question arises, Which is the best excitation light for a given LSPR position? For a long time, it was believed that the best excitation for a given LSPR was light that perfectly matched the LSPR maximum. Later on, and supported by experimental observations, it was believed that it was better to use an excitation light that was slightly red-shifted from the maximum of the plasmon extinction spectrum.[17] The answer however was given by Van Duyne by means of surface-enhanced Raman excitation spectroscopy (SERES).[18] In this report, perfectly organized and homogeneous silver thin films with different optical response, from the blue to the NIR, were coated with a monolayer of BT and sampled with 13 different excitation lights (Figure 4B). The simultaneous representation of the LSPR extinction spectra and the enhancement factor (EF) obtained for each excitation line showed in all cases that the best excitation was a little blue-shifted with respect to the LSPR maximum. This fact is in full agreement with the electromagnetic mechanism, which predicts that maximum SERS intensity is achieved when the LSPR strongly enhances both the incident and scattered photon intensities.[5] This paper also explained the wrong perception that the best EF was obtained by exciting the sample at the red of the plasmon by characterizing the optical properties of the film before and after retention of BT. Figure 3B shows how the plasmon red shifts 57 nm after retention of the

dx.doi.org/10.1021/jz201625j | J. Phys. Chem. Lett. 2012, 3, 857−866

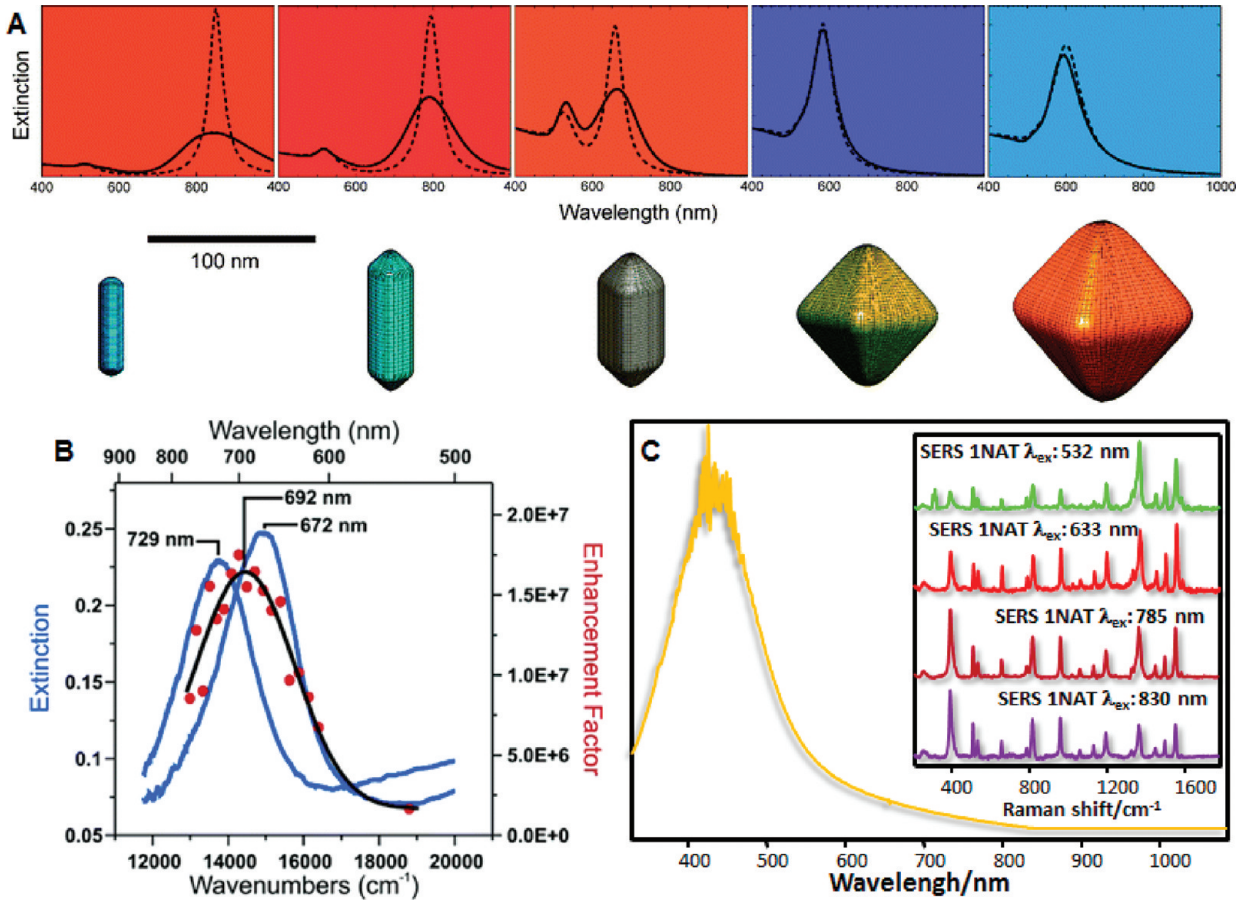

Figure 4. (A) Controlled growth of small circular gold rods (left) to large octahedra through intermediate stages involving square rods of decreasing aspect ratio and small octahedra. Experimental (solid curves) and theoretical (dotted curves) LSPR spectra. The particles are painted here in the colors of the light that they scatter when illuminated with a white source. The background color in each plot corresponds to the light transmitted through a dilute colloidal dispersion. (B) LSPR shift and SERES profile for the ring stretch (1575 cm^{-1}) of BT. The line with λ_{max} = 672 nm is the LSPR extinction of the bare nanoparticle array. The line with λ_{max} = 729 nm is the LSPR extinction of the nanoparticle array with an adsorbed monolayer of BT. The line with $\lambda_{ex,max}$ = 692 nm is the best fit to the SERES data points. (C) LSPR spectra and SERS spectra with different excitation lights of 1-naphthalenethiol on an exponentially growth layer-by-layer film containing silver nanoparticles. Reproduced with permission from refs 16, 18, and 19. Copyright 2008, Royal Society for Chemistry; 2005, American Chemical Society; and 2009, Wiley-VCH.

analyte, with maximum EF placed in between. Thus, while SERES observations are true, the experimental observations that the red excitation will yield the best EF are also true, pointing out the importance of the characterization of the LSPR before and after the addition of the analyte to avoid confusion.

> The simultaneous representation of the LSPR extinction spectra and the enhancement factor (EF) obtained for each excitation line showed in all cases that the best excitation was a little blue-shifted with respect to the LSPR maximum.

Another typical observation is the obtainment of good-quality SERS spectra on optical enhancers that present a LSPR far away from the excitation laser lines. A characteristic example of this can be observed in Figure 4C, where a thin film composed of silver nanoparticles and characterized by a strong LSPR between 400 and 600 nm yields extremely good SERS spectra with excitation lines at 785 and 830 nm. Besides the (small) red shift due to analyte retention, the natural explanation of this fact is the formation of randomly distributed hot spots. The LSPR of these hot spots cannot be easily determined as their proportion in the sample is low. However, hot spots are very optically active and can yield EFs over 5 orders of magnitude as compared with those of regular particles.[20]

The last factor to be considered is the composition of the nanoparticles. In this case, although SERS has been reported for many metals, the vast majority of studies and applications are developed with gold and silver. Here, it is important to note that though gold has some advantages over silver (i.e., chemical stability and more biocompatibility), silver is a much more efficient optical enhancer, and for the same particle size and shape, it yields EFs 2 or 3 orders of magnitude larger than those of gold.[21] Further, due to the presence of interband transitions near the green for gold, it can be only efficiently excited from the red onward, while silver can be used as well for applications requiring excitations at the green of even the blue.[22]

dx.doi.org/10.1021/jz201625j | J. Phys. Chem. Lett. 2012, 3, 857–866

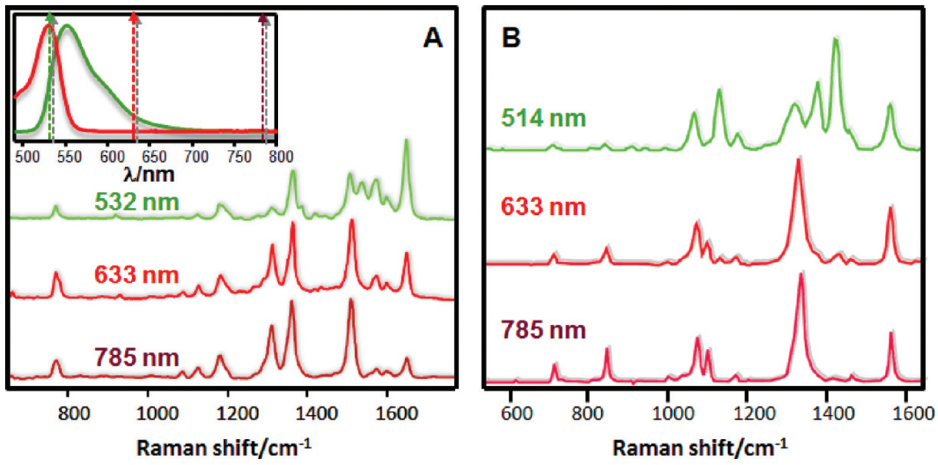

Figure 5. (A) SERRS and SERS spectra of R6G and (B) pre-SERRS and SERS spectra of *p*-nitroBT, both on silver colloids and upon excitation with different laser lines, from the green to the NIR.

Analyte Molecule. Problems such as background fluorescence, photocatalysis, sample degradation, and thermal heating, which leads to diffusion or sublimation, are ubiquitous in Raman. In SERS, and due to the presence of the metallic nanostructures, which often form a chemical complex with the analyte, some of these problems get solved, while others are exacerbated.

Double Resonance. Fluorescence occurs when the HOMO−LUMO transition of the analyte is excited with the appropriate light (the excitation wavelength overlaps the electronic absorption of the molecule). Then, the excited electron relaxes to its ground state by emitting a photon of light. When a metallic surface is in close proximity, the fluorescence emission decays as the excited electron is deactivated by surface energy transfer, a nonradiative mechanism. When the metallic surface is a plasmonic nanoparticle and is irradiated to get SERS, the double resonance excitation (i.e., the plasmon and the electronic absorption band of the analyte) yields a very intense scattering, especially for those vibrational modes related to the chromophore.[23] This phenomenon, known as surface-enhanced resonance Raman scattering (SERRS), has two net effects. The first is the increase in the intensity, up to 5 orders of magnitude as compared to that of SERS, of the vibrational spectrum; the second is the change in the vibrational profile of the spectrum. SERRS has a deep impact in the ultrasensitive analysis where a dye is involved. The SERRS and SERS spectra of rhodamine 6G (R6G) obtained from silver colloids are illustrated in Figure 5A. The absorption spectrum of R6G (inset, Figure 4A) exhibits a band in the visible region from 440 to 560 nm, with a maximum at 527 nm, in nearly perfect resonance with the 532 nm excitation line but far away from the red and NIR excitations. Conversely, SERS spectra obtained from the red and NIR lines present a similar vibrational profile, while the SERRS spectra, acquired with the green line, notably differ. Notably, both spectra SERS and SERRS contain the same vibrational features but with different relative intensity. As expected, the more-enhanced modes in SERRS results in the chromophore (xantene ring) with stretching contributions, especially those at 1650 and 1572 cm^{-1}, while the less-enhanced band corresponds to an in-plane ring bending (1311 cm^{-1}) that very probably quenches the electronic resonance.[24]

In the case of surface complexation, electronic absorption of the complexed analyte may shift with respect to the free molecule, overlapping the excitation wavelength. This is commonly referred to in the literature as the chemical SERS effect.[9] Figure 5B shows the SERS spectra of *p*-nitroBT on silver colloids for three excitations, 514, 633, and 785 nm. The relative intensities in the spectrum recorded with the 514 nm laser line are different from those obtained by exciting in the red and the NIR. There may be two explanations for the variation of the relative intensities in the spectra as the energy of the laser increases. First, for a well-oriented chemisorbed species, the perpendicular and tangential components of the local field on the silver colloids could be quite different in magnitude for laser lines on different sides of the plasmon resonance.[25] Therefore, relative intensities will vary according to the orientation of the polarizability derivatives and the magnitude of the local field at the surface. The alternative explanation considers the possibility of a charge-transfer Ag complex with an electronic absorption in the spectral region of the exciting lines. The UV−vis spectrum of this analyte shows a strong absorption at 223 nm, very far from the green to have any resonant effect. However, the electronic spectrum of the analyte complexed with silver shows as well a broad shoulder that extends up to the 500 nm region. The 514 nm laser line is thus in preresonance with the absorption of the complex, and this explains the variation in relative intensities observed with this particular laser line. Because the variation in relative intensities is also observed with the isolated complex, it can be concluded that a charge-transfer absorption band is responsible for the peculiar relative intensity pattern observed in the SERS of *p*-nitroBT as a function of the excitation energy.[26]

Upon excitation with intense light and with the generation of such strong electric fields at their surface (i.e., LSPR), it is not unusual that these materials may lead to photocatalytically induced reactions.

Photocatalysis. As previously stated, SERS is always carried out in the presence of plasmonic enhancers. These enhancers

dx.doi.org/10.1021/jz201625j | *J. Phys. Chem. Lett.* 2012, 3, 857−866

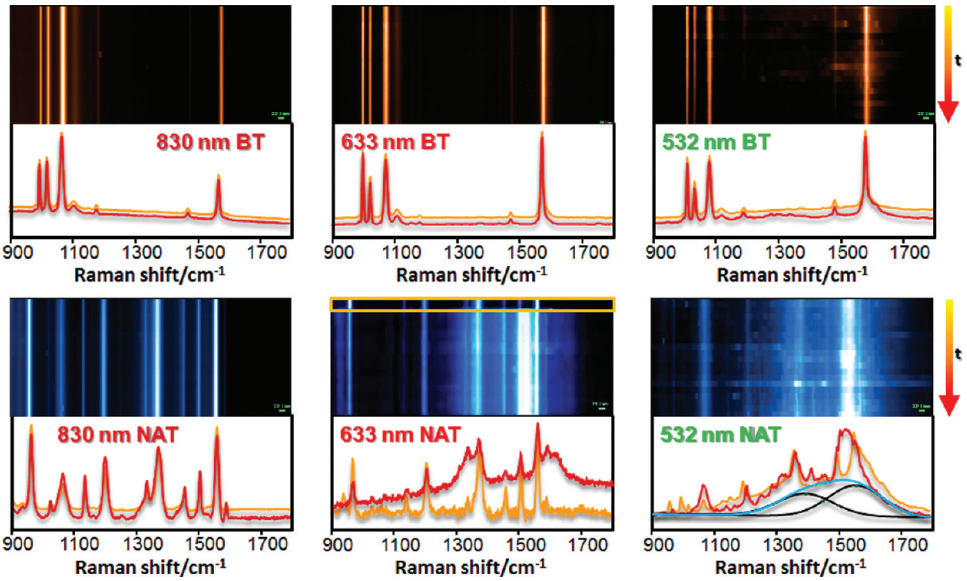

Figure 6. SERS spectra of BT and 1NAT on a silver island film acquired after irradiation of the same spot for 1470 s (time step was 30 s) with different laser lines (×50, ~15 μW). The yellow spectrum represents the initial acquisition at time 0; the red spectrum represents the result at time 1470 s. The blue and black lines, in the case of 1NAT under irradiation with a green laser, illustrate the amorphous carbon background due to the photocombustion of the sample. The panels over the spectra represent the variation of the spectral profile with the irradiation time.

are usually made of gold and silver, and these metals are intrinsically good catalysts for different types of reactions. Upon excitation with intense light and with the generation of such strong electric fields at their surface (i.e., LSPR), it is not unusual that these materials may lead to photocatalytically induced reactions. Some of these reactions are well-known, for example, the photoreduction of methyl viologen, the photodecomposition of azo-compounds, or the photoisomerization of maleic acid. Photocatalytic changes induced in the analyte by the laser have to be considered, especially when the obtained SERS spectrum cannot be explained on the basis of the Raman spectrum, and the vibrational profile with a given wavelength is different from those obtained with other laser lines. For example, when acquiring the SERS spectrum of 4-nitrobenzenethiol on nanostructured silver in static conditions and with a green laser, the spectrum obtained corresponds to 4-aminobenzenethiol. To avoid this photoinduced reduction, the spectra should be acquired in solution, if possible with recirculation, or with a NIR line.[27]

Photodegradation. In static enhancing systems such as island films, cast colloids, and other solid nanomaterials, sample damage by exposure to the laser is frequent. In fact, it has been an endemic problem in SERS since its origins.[28] The most common example is the formation of graphitic or amorphous carbon, giving rise to the undesired sp^2 stretchings (1360 and 1560 cm^{-1}) also known as "cathedral bands".[29] Photodegradation can be considered as a particular photocatalytic process in which the precursor molecule (the analyte) is transformed into amorphous carbon upon excitation with visible lines.[30] Amorphous carbon not only has a very high Raman cross section, nearly four-times that of benzene, but also a varying degree of molecular resonance throughout the electromagnetic spectrum, from the UV to the NIR.[31] This variation has been attributed to the modification of graphitic-like carbon, both structurally and chemically, as it interacts with its environment. The generation of this spurious carbon depends strongly on the excitation energy, the energy density at the sample, and the chemical nature of the analyte. To illustrate these factors, Figure 6 shows the behavior with time of two different analytes, BT and 1-naphthalenethiol (1NAT).

BT shows great photostability from the NIR to the green. For all laser lines, its characteristic vibrational modes can be easily identified at both the initial time and after irradiation for more than 20 min. In fact, the formation of spurious species due to the sample photocombustion can only be very slightly observed after irradiation with the shorter wavelength (532 nm) over several minutes (see the appearance of the color, especially around the ring stretching at 1575 cm^{-1} in the panel over the spectra in Figure 6). 1NAT, however, is only stable under irradiation with the NIR laser. Notably, when the energy is increased to 633 nm, the molecule is only stable for a couple of minutes (highlighted in yellow in the panel), which usually allows sufficient time to record a high-quality spectrum. The formation of amorphous carbon species after this time is evident. It is worth noting that after 23 min of irradiation, the characteristic vibrational modes of 1NAT can still be identified, which indicates that the extension of combustion is still limited. Excitation with the green laser yields to combustion since the beginning, however, in this case, the destruction of the molecule is quite rapid, with no identifiable 1NAT bands after 30 s.

Several strategies can be applied to avoid photocombustion. Some often commented involve defocusing the sample or changing the objective to lower magnifications. However, by doing this, irradiation of the sample will still be almost the same, while the inelastically scattered light collected at the detector will decrease enormously. Other more promising alternatives consist of reducing the flux of photons to the sample by either decreasing the laser power, decreasing the acquisition time, or both. However, the best alternative is always switching the excitation to longer wavelengths and, if necessary, to acquire the spectrum with a given laser but in colloidal solution where Brownian motion will avoid the illumination of the same part of the sample while the liquid will dissipate heat and thus attenuate the effects of the radiation.

Thermal Heating. An issue that is a concern in any Raman experiment is the laser-induced local heating. Measured laser

dx.doi.org/10.1021/jz201625j | J. Phys. Chem. Lett. 2012, 3, 857–866

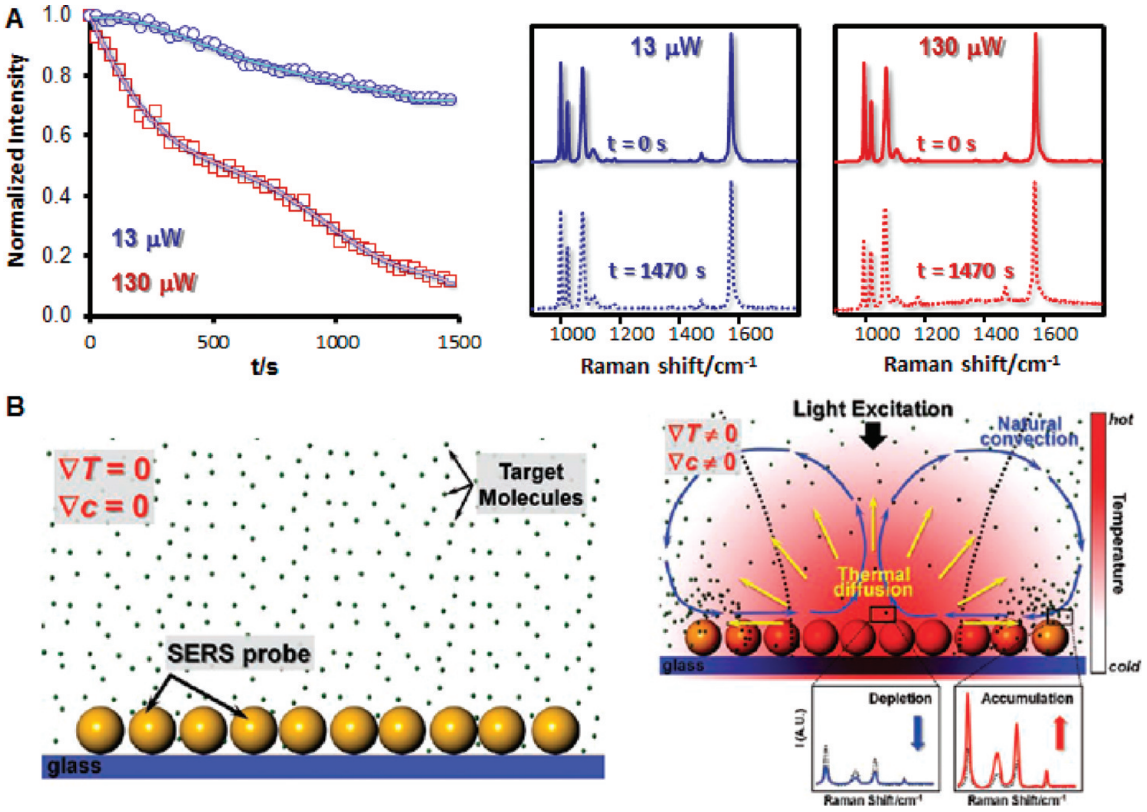

Figure 7. (A) Thermal behavior of a BT monolayer on a silver island film under irradiation with a red laser (633 nm) on the same spot as a function of the power at the sample and the time. (B) The schematics of the thermophoretic effect in SERS. The target molecule distribution and SERS probe array before light excitation. T and c represent the temperature and concentration of the target molecules, respectively. The redistribution of the molecules by thermal diffusion and natural convection upon exposure of the excitation light source. The SERS intensity changes by the thermophoretic effect are schematically illustrated at a depleted and accumulated position. When the excitation source is illuminated to precipitated gold nanoparticles, a temperature gradient is generated by the absorption of the incident light. The gradient leads to targeting of the molecules to move. Blue and yellow arrows represent fluidic convection motion and thermal diffusion induced by the temperature gradient. (B) is adapted with permission from ref 37. Copyright 2010, Wiley-VCH.

heating shows very small temperature changes (0.1 K for an energy density of 1 μW) with the energy densities typically used in SERS.[32] However, with the presence of metallic nanoparticles that absorb the radiation, the situation changes.[33] As the plasmonic substrate is irradiated, its temperature may increase up to levels where sublimation of the sample is possible. This process depends of course on the density energy at the sample, the irradiation time, and the nature of the retained molecule. Figure 7A shows the thermal effects of a BT monolayer on a silver island film coated with a monolayer of BT under irradiation with a red laser on the same spot as a function of the power at the sample and irradiation time. For low power at the sample (13 μW), a decrease in the SERS intensity can be observed with time. This decrease is constant, and both spectra, initial and after irradiation for 23 min, show exactly the same vibrational profile, with a loss of intensity of about 20% but without any evidence of carbon formation. If the experiment is repeated at a different spot but with increasing energy (130 μW), the result is similar but with a signal loss of 90%. Although in this case carbon formation cannot be appreciated, comparison between the spectra at t = 0 and after 1470 s shows a different relative intensity distribution for the bands due to the ring breathings (999 and 1073 cm^{-1}) and the CH in-plane bending (1023 cm^{-1}). These variations can be discussed in light of the surface selection rules[34] and point toward a different molecular orientation of the remaining BT adsorbed molecules on the film as the monolayer gets less packed.[35] This supports as well the photosublimation of BT as the cause for the loss of intensity.

When the analyte molecules are nonvolatile, a thermal breakdown can occur as well. In this case, the signal decay is ascribed to the molecular diffusion of the molecules across the plasmonic surfaces.[36,37] This effect is especially noticeable in experiments where the analyte concentration is ultralow, such as those in or near the single-molecule regime.

Most of these undesired effects can be notably reduced or even avoided by carrying out the SERS experiment at low temperature.[38] In general, decreasing the sample temperature has several desirable effects, such as a sharp decrease of the band broadening,[39] less sample degradation due to laser damage, better analyte adsorption, and a suppression of analyte diffusion. Additionally, the acquisition of the SERS spectra in vacuum or in inert atmospheres usually improves the signal-to-noise ratio, as well as reducing the spectral fluctuations and the reactivity of the analyte toward the generation of new species.

SERS is nowadays a well-established ultrasensitive technique with the potential to solve many analytical problems, especially those related to biosciences. Still, most of the developed applications rely on the identification of well-known vibrational patterns. Thus, a tremendous effort still needs to be given in order to understand the enhanced vibrational spectrum, so that predictions can be made and/or the unknown components

dx.doi.org/10.1021/jz201625j | J. Phys. Chem. Lett. 2012, 3, 857–866

in a sample can be identified. To achieve this objective, the publication of the correct vibrational features associated with a given analyte in a given situation is essential. It is indispensable for the SERS practitioner to understand the theoretical basis underlying the effect, and it is crucial to know the experimental variables associated with the technique, especially those related to the interaction of the excitation light with the sample. A systematic description of these factors and hopefully the generation of a SERS spectral library describing the particular conditions under which the experiment has been carried out will be of tremendous help toward the use of these powerful analytical methods for practical applications.

AUTHOR INFORMATION

Corresponding Author

*E-mail: ramon.alvarez@uvigo.es.

Notes

The authors declare no competing financial interest.

Biography

Ramón A. Alvarez-Puebla is currently a Research Scientist at the Department of Physical Chemistry, University of Vigo. He worked as a postdoc in the Department of Chemistry and Biochemistry of the University of Windsor (Canada) with Prof. Ricardo Aroca, and he was appointed as Research Officer at the National Institute for Nanotechnology of the National Research Council of Canada. He has coauthored over 90 articles and holds 2 patents. His current interests involve electronic and vibrational spectroscopy, surface-enhanced spectroscopy, and its application in sensing and chemical biology.

ACKNOWLEDGMENTS

This work has been supported by the Spanish MICINN (MAT2008-05755 and CTQ2011-23167).

REFERENCES

(1) Aroca, R. F. *Surface-Enhanced Vibrational Spectroscopy*; Wiley-VCH: Weinheim, Germany, 2006.
(2) Alvarez-Puebla, R. A.; Liz-Marzan, L. M. Environmental Applications of Plasmon Assisted Raman Scattering. *Energy Environ. Sci.* **2010**, *3*, 1011−1017.
(3) Kho, K. W.; Fu, C. Y.; Dinish, U. S.; Olivo, M. Clinical SERS: Are We There Yet? *J. Biophoton.* **2011**, *4*, 667−684.
(4) Moskovits, M. Surface-Enhanced Raman Spectroscopy: A Brief Retrospective. *J. Raman Spectrosc.* **2005**, *36*, 485−496.
(5) Stiles, P. L.; Dieringer, J. A.; Shah, N. C.; Van Duyne, R. P. Surface-Enhanced Raman Spectroscopy. *Annu. Rev. Anal. Chem.* **2008**, *1*, 601−626.
(6) Willets, K. A.; Van Duyne, R. P. Localized Surface Plasmon Resonance Spectroscopy and Sensing. *Annu. Rev. Phys. Chem.* **2007**, *58*, 267−297.
(7) Morton, S. M.; Silverstein, D. W.; Jensen, L. Theoretical Studies of Plasmonics using Electronic Structure Methods. *Chem. Rev.* **2011**, *111*, 3962−3994.
(8) Campion, A.; Kambhampati, P. Surface-Enhanced Raman Scattering. *Chem. Soc. Rev.* **1998**, *27*, 241−250.
(9) Otto, A. The 'Chemical' (Electronic) Contribution to Surface-Enhanced Raman Scattering. *J. Raman Spectrosc.* **2005**, *36*, 497−509.
(10) Ren, B.; Lin, X.-F.; Yang, Z.-L.; Liu, G.-K.; Aroca, R. F.; Mao, B.-W.; Tian, Z.-Q. Surface-Enhanced Raman Scattering in the Ultraviolet Spectral Region: UV−SERS on Rhodium and Ruthenium Electrodes. *J. Am. Chem. Soc.* **2003**, *125*, 9598−9599.
(11) Born, M.; Wolf, E. *Principles of Optics*, 6th ed.; Pergamon Press: Oxford, U.K., 1980.
(12) Ray, K. G.; McCreery, R. L. Simplified Calibration of Instrument Response Function for Raman Spectrometers Based on Luminescent Intensity Standards. *Appl. Spectrosc.* **1997**, *51*, 108−116.
(13) Grzelczak, M.; Perez-Juste, J.; Mulvaney, P.; Liz-Marzan, L. M. Shape Control in Gold Nanoparticle Synthesis. *Chem. Soc. Rev.* **2008**, *37*, 1783−1791.
(14) Xia, Y. N.; Li, W. Y.; Cobley, C. M.; Chen, J. Y.; Xia, X. H.; Zhang, Q.; Yang, M. X.; Cho, E. C.; Brown, P. K. Gold Nanocages: From Synthesis to Theranostic Applications. *Acc. Chem. Res.* **2011**, *44*, 914−924.
(15) Romo-Herrera, J. M.; Alvarez-Puebla, R. A.; Liz-Marzan, L. M. Controlled Assembly of Plasmonic Colloidal Nanoparticle Clusters. *Nanoscale* **2011**, *3*, 1304−1315.
(16) Myroshnychenko, V.; Rodriguez-Fernandez, J.; Pastoriza-Santos, I.; Funston, A. M.; Novo, C.; Mulvaney, P.; Liz-Marzan, L. M.; Garcia de Abajo, F. J. Modelling the Optical Response of Gold Nanoparticles. *Chem. Soc. Rev.* **2008**, *37*, 1792−1805.
(17) Alvarez-Puebla, R. A.; Ross, D. J.; Nazri, G. A.; Aroca, R. F. Surface-Enhanced Raman Scattering on Nanoshells with Tunable Surface Plasmon Resonance. *Langmuir* **2005**, *21*, 10504−10508.
(18) McFarland, A. D.; Young, M. A.; Dieringer, J. A.; Van Duyne, R. P. Wavelength-Scanned Surface-Enhanced Raman Excitation Spectroscopy. *J. Phys. Chem. B* **2005**, *109*, 11279−11285.
(19) Abalde-Cela, S.; Ho, S.; Rodriguez-Gonzalez, B.; Correa-Duarte, M. A.; Alvarez-Puebla, R. A.; Liz-Marzan, L. M.; Kotov, N. A. Loading of Exponentially Grown LBL Films with Silver Nanoparticles and Their Application to Generalized SERS Detection. *Angew. Chem., Int. Ed.* **2009**, *48*, 5326−5329.
(20) Alvarez-Puebla, R.; Liz-Marzán, L. M.; García de Abajo, F. J. Light Concentration at the Nanometer Scale. *J. Phys. Chem. Lett.* **2010**, *1*, 2428−2434.
(21) García de Abajo, F. J. Light Scattering by Particle and Hole Arrays. *Rev. Mod. Phys.* **2007**, *79*, 1267−1290.
(22) Zhao, J.; Pinchuk, A. O.; McMahon, J. M.; Li, S.; Ausman, L. K.; Atkinson, A. L.; Schatz, G. C. Methods for Describing the Electromagnetic Properties of Silver and Gold Nanoparticles. *Acc. Chem. Res.* **2008**, *41*, 1710−1720.
(23) McNay, G.; Eustace, D.; Smith, W. E.; Faulds, K.; Graham, D. Surface-Enhanced Raman Scattering (SERS) and Surface-Enhanced Resonance Raman Scattering (SERRS): A Review of Applications. *Appl. Spectrosc.* **2011**, *65*, 825−837.
(24) Jensen, L.; Schatz, G. C. Resonance Raman Scattering of Rhodamine 6G as Calculated Using Time-Dependent Density Functional Theory. *J. Phys. Chem. A* **2006**, *110*, 5973−5977.
(25) Moskovits, M. Surface-Enhanced Spectroscopy. *Rev. Mod. Phys.* **1985**, *57*, 783−826.
(26) Skadtchenko, B. O.; Aroca, R. Surface-Enhanced Raman Scattering of p-Nitrothiophenol: Molecular Vibrations of Its Silver Salt and the Surface Complex Formed on Silver Islands and Colloids. *Spectrochim. Acta, Part A* **2001**, *57*, 1009−1016.
(27) Kim, K.; Lee, S. J.; Kim, K. L. Surface-Enhanced Raman Scattering of 4-Nitrothioanisole in Ag Sol. *J. Phys. Chem. B* **2004**, *108*, 16208−16212.
(28) Cooney, R. P.; Howard, M. W.; Mahoney, M. R.; Mernagh, T. P. Chemical Reactivity and Surface-Enhanced Raman Scattering. *Chem. Phys. Lett.* **1981**, *79*, 459−464.
(29) Otto, A. What Is Observed in Single Molecule SERS, and Why? *J. Raman Spectrosc.* **2002**, *33*, 593−598.
(30) Bjerneld, E. J.; Svedberg, F.; Johansson, P.; Käll, M. Direct Observation of Heterogeneous Photochemistry on Aggregated Ag Nanocrystals Using Raman Spectroscopy: The Case of Photoinduced Degradation of Aromatic Amino Acids. *J. Phys. Chem. A* **2004**, *108*, 4187−4193.
(31) Ferrari, A. C.; Robertson, J. Resonant Raman Spectroscopy of Disordered, Amorphous, And Diamondlike Carbon. *Phys. Rev. B* **2001**, *64*, 075414.
(32) Weiss, A.; Haran, G. Time-Dependent Single-Molecule Raman Scattering as a Probe of Surface Dynamics. *J. Phys. Chem. B* **2001**, *105*, 12348−12354.
(33) Viets, C.; Hill, W. Laser Power Effects in SERS Spectroscopy at Thin Metal Films. *J. Phys. Chem. B* **2001**, *105*, 6330−6336.

(34) Moskovits, M.; Suh, J. S. Surface Selection-Rules for Surface-Enhanced Raman-Spectroscopy — Calculations and Application to the Surface-Enhanced Raman-Spectrum of Phthalazine on Silver. *J. Phys. Chem.* **1984**, *88*, 5526−5530.
(35) Moskovits, M.; Dilella, D. P.; Maynard, K. J. Surface Raman-Spectroscopy of a Number of Cyclic Aromatic-Molecules Adsorbed on Silver — Selection-Rules and Molecular-Reorientation. *Langmuir* **1988**, *4*, 67−76.
(36) Maruyama, Y.; Ishikawa, M.; Futamata, M. Thermal Activation of Blinking in SERS Signal. *J. Phys. Chem. B* **2003**, *108*, 673−678.
(37) Kang, T.; Hong, S.; Choi, Y.; Lee, L. P. The Effect of Thermal Gradients in SERS Spectroscopy. *Small* **2010**, *6*, 2649−2652.
(38) Pang, Y. S.; Hwang, H. J.; Kim, M. S. Reversible Temperature Dependence in Surface-Enhanced Raman Scattering of 1-Propanethiol Adsorbed on a Silver Island Film. *J. Phys. Chem. B* **1998**, *102*, 7203−7209.
(39) Artur, C.; Le Ru, E. C.; Etchegoin, P. G. Temperature Dependence of the Homogeneous Broadening of Resonant Raman Peaks Measured by Single-Molecule Surface-Enhanced Raman Spectroscopy. *J. Phys. Chem. Lett.* **2011**, *2*, 3002−3005.